

Quantum dust cores of rotating black holes

Tommaso Bambagiotti^{ab*} and Roberto Casadio^{abc†}

^a*Dipartimento di Fisica e Astronomia, Università di Bologna
via Irnerio 46, 40126 Bologna, Italy*

^b*I.N.F.N., Sezione di Bologna, I.S. FLAG
viale B. Pichat 6/2, 40127 Bologna, Italy*

^c*Alma Mater Research Center on Applied Mathematics (AM²)
Via Saragozza 8, 40123 Bologna, Italy*

January 6, 2026

Abstract

A quantum description of dust cores for black hole geometries can be obtained by quantising the geodesic motion of dust particles and finding the corresponding many-body ground state. We here generalise previous works in spherical symmetry to rotating geometries and show the effect of angular momentum on the size of the core and effective interior geometry.

1 Introduction

The singularities of known black hole solutions of the Einstein equations [1] can be removed by imposing regularity conditions on the (effective) energy density and scalar invariants inspired by classical physics [2]. This procedure usually induces the appearance (or fails to remove) an inner Cauchy horizon. A different framework, invoked for example in Ref. [3], can be implemented based on the possibility that black hole interiors and the collapsed matter therein are described more accurately by quantum physics. One can then consider an effective energy density $\rho \sim |\psi|^2$, where $\psi = \psi(r)$ is the wavefunction of the collapsed matter source, such that the Misner-Sharp-Hernandez (MSH) mass function [4, 5] satisfies

$$m(r) \equiv 4\pi \int_0^r \rho(x) x^2 dx \sim 4\pi \int_0^r |\psi(x)|^2 x^2 dx < \infty \quad \text{for } r > 0. \quad (1.1)$$

This accommodates for $\rho \sim r^{-2}$ and $m \sim r$, which ensures that $m(0) = 0$ and replaces the central singularity with an integrable singularity [6, 7], that is a region where the curvature invariants and the effective energy-momentum tensor diverge but their volume integrals remain finite [8]. Additionally, no inner horizon is present.

*E-mail: tommaso.bambagiotti2@unibo.it

†E-mail: casadio@bo.infn.it

An explicit realisation for the inner core of a quantum Schwarzschild black hole based on the Oppenheimer-Snyder model of dust collapse [9] was analysed in Ref. [10] (see also Refs. [11, 12]). The ball was described as a sequence of layers [13] containing dust particles, whose trajectories are individually quantised. A condition was then imposed to ensure that the fuzzy quantum layers defined by the positions of these particles remain orderly nested in the global quantum ground state, which confirmed the expected quantum behaviour in Eq. (1.1) for the effective energy density and mass function [10, 14]. The same approach was then applied to the Reissner-Nordström geometry in Ref. [15], with similar results about the absence of inner horizons.

In this work we will consider (differentially) rotating cores of dust by explicitly employing geodesic motion in the (generalised) Kerr metric and compare with the perturbative results of Ref. [16], where angular momentum was added to the spherical symmetric geometry. We will find that the fully general relativistic treatment leads to elongated dust cores compared to the spherically symmetric case. We will also identify a configuration in which the effective mass function and specific angular momentum grow linearly inside the dust core, as expected for an integrable singularity without Cauchy horizons of the form discussed in Ref. [3].

2 Rotating geodesics

We will describe the collapsing matter as dust particles moving in a generalised Kerr geometry which, in Boyer-Lindquist coordinates $x^\alpha = (t, r, \theta, \phi)$, reads ¹

$$ds^2 = -dt^2 + \frac{2G_N m r}{\rho^2} (a \sin^2 \theta d\phi - dt)^2 + \rho^2 \left(\frac{dr^2}{\Delta} + d\theta^2 \right) + (r^2 + a^2) \sin^2 \theta d\phi^2 , \quad (2.1)$$

where

$$\rho^2 = r^2 + a^2 \cos^2 \theta \quad (2.2)$$

and

$$\Delta = r^2 - 2G_N m r + a^2 . \quad (2.3)$$

In the above expressions, the function $m = m(r)$ represents the MSH mass inside ellipsoids of coordinate radius r and $a = a(r) = J(r)/m(r)$ is the specific angular momentum on the surface of the same ellipsoid [3].

We recall that the vacuum Kerr metric is given by constant $a = A$ and $m = M$, where M is now the Arnowitt-Deser-Misner (ADM) mass [17], and it contains horizons located at

$$R_\pm = G_N M \pm \sqrt{G_N^2 M^2 - A^2} , \quad (2.4)$$

provided $A^2 \leq G_N^2 M^2$. We expect m and a to approach asymptotically M and A , respectively, in the vacuum outside the collapsing dust.

¹We shall always use units with $c = 1$ and often write the Planck constant $\hbar = \ell_p m_p$ and the Newton constant $G_N = \ell_p/m_p$, where ℓ_p and m_p are the Planck length and mass, respectively.

2.1 Action and equations of motion

Assuming individual dust particles have a proper mass $\mu \ll m$, their trajectories can be approximated by time-like geodesics $x^\alpha = x^\alpha(\tau)$ in the metric (2.1), governed by the Lagrangian

$$2L = \dot{t}^2 - \frac{2G_N m r}{\rho^2} \left(a \sin^2 \theta \dot{\phi} - \dot{t} \right)^2 - \rho^2 \left(\frac{\dot{r}^2}{\Delta} + \dot{\theta}^2 \right) - (r^2 + a^2) \sin^2 \theta \dot{\phi}^2 , \quad (2.5)$$

which yields the mass-shell condition $2L = 1$ and the integrals of motion

$$\frac{E}{\mu} = \left(1 - \frac{2G_N m r}{\rho^2} \right) \dot{t} + \frac{2G_N m a r}{\rho^2} \sin^2 \theta \dot{\phi} \quad (2.6)$$

and

$$j = \left(r^2 + a^2 + \frac{2G_N m a^2 r}{\rho^2} \sin^2 \theta \right) \sin^2 \theta \dot{\phi} - \frac{2G_N m a r}{\rho^2} \sin^2 \theta \dot{t} . \quad (2.7)$$

We can invert the above relations and obtain

$$\begin{aligned} \dot{t} &= \frac{1}{\Delta} \left[\left(r^2 + a^2 + \frac{2G_N m a^2 r}{\rho^2} \sin^2 \theta \right) \frac{E}{\mu} - \frac{2G_N m a r}{\rho^2} j \right] \\ &= \frac{E}{\mu} + \frac{4G_N m r [(r^2 + a^2) E/\mu + a j]}{(r^2 + a^2 - 2G_N m r) [2r^2 + a^2 (1 + \cos 2\theta)]} \end{aligned} \quad (2.8)$$

and

$$\begin{aligned} \dot{\phi} &= \frac{1}{\Delta} \left[\left(\frac{2G_N m a r}{\rho^2} \right) \frac{E}{\mu} + \left(1 - \frac{2G_N m r}{\rho^2} \right) \frac{j}{\sin^2 \theta} \right] \\ &= \frac{4G_N m a r E/\mu + 2a^2 j}{(r^2 + a^2 - 2G_N m r) [2r^2 + a^2 (1 + \cos 2\theta)]} - \frac{2j}{[2r^2 + a^2 (1 + \cos 2\theta)] \sin^2 \theta} . \end{aligned} \quad (2.9)$$

We next assume that the dust particles in a layer at the surface of an ellipsoid of radial coordinate $r = r(\tau)$ co-rotate with the geometry and therefore have $j = 0$, that is

$$\left(r^2 + a^2 + \frac{2G_N m a^2 r}{\rho^2} \sin^2 \theta \right) \dot{\phi} = \frac{2G_N m a r}{\rho} \dot{t} , \quad (2.10)$$

which implies

$$\begin{aligned} \dot{t} &= \left[1 + \frac{2G_N m r (r^2 + a^2)}{\Delta \rho^2} \right] \frac{E}{\mu} \\ &= \left\{ 1 + \frac{4G_N m r (r^2 + a^2)}{(r^2 + a^2 - 2G_N m r) [2r^2 + a^2 (1 + \cos 2\theta)]} \right\} \frac{E}{\mu} \end{aligned} \quad (2.11)$$

and

$$\begin{aligned} \dot{\phi} &= \left(\frac{2G_N m a r}{\Delta \rho^2} \right) \frac{E}{\mu} \\ &= \frac{4G_N m a r E/\mu}{(r^2 + a^2 - 2G_N m r) [2r^2 + a^2 (1 + \cos 2\theta)]} . \end{aligned} \quad (2.12)$$

With this assumption, the Lagrangian (2.5) simplifies to

$$2L_0 = -\rho^2 \left(\frac{\dot{r}^2}{\Delta} + \dot{\theta}^2 \right) + \left[1 + \frac{2G_N m r (r^2 + a^2)}{\Delta \rho^2} \right]^2 \frac{E^2}{\mu^2} - \left[\frac{2G_N m r (r^2 + a^2)}{\Delta^2 \rho^2} \right] \frac{E^2}{\mu^2} + \left[\frac{4G_N^2 m^2 a^2 r^2 (r^2 + a^2) \sin^2 \theta}{\Delta^2 \rho^2} \right] \frac{E^2}{\mu^2} = 1. \quad (2.13)$$

We note that, for the ground state $E^2 = 0$, the above expression greatly simplifies to

$$2L_0 = -\rho^2 \left(\frac{\dot{r}^2}{\Delta} + \dot{\theta}^2 \right) = 1, \quad (2.14)$$

which can be written as

$$\frac{1}{2} \dot{r}^2 + \frac{\Delta}{2\rho^2} + \frac{\Delta}{2} \dot{\theta}^2 = \frac{1}{2} \dot{r}^2 + \frac{r^2 - 2G_N m r + a^2}{2(r^2 + a^2 \cos^2 \theta)} + \frac{1}{2} (r^2 - 2G_N m r + a^2) \dot{\theta}^2 = 0. \quad (2.15)$$

The equation of motion for $\theta = \theta(\tau)$ then reads

$$\ddot{\theta} = \frac{1}{2} \frac{\partial}{\partial \theta} \left(\frac{1}{r^2 + a^2 \cos^2 \theta} \right) = \frac{a^2 \cos \theta \sin \theta}{(r^2 + a^2 \cos^2 \theta)^2}, \quad (2.16)$$

so that $\theta = \theta(\tau)$ can be constant in the ground state with $E = j = 0$ only for $\theta = 0$ or $\theta = \pi/2$.

Let us next consider the case of radial motion along the axis of symmetry $\theta = \dot{\theta} = 0$, and motion on the equatorial plane $\theta = \pi/2$ and $\dot{\theta} = 0$.

2.1.1 Axial motion

For $\theta = \dot{\theta} = 0$, the Lagrangian (2.13) reads

$$2L_0 = \left(1 - \frac{2G_N m r}{\rho^2} \right)^{-1} \frac{E^2}{\mu^2} - \frac{\rho^2}{\Delta} \dot{r}^2 = 1, \quad (2.17)$$

which can be written as

$$\frac{1}{2} \mu \dot{r}^2 - \frac{G_N \mu m}{r} \left(1 - \frac{a^2}{r^2 + a^2} \right) = \frac{\mu}{2} \left(\frac{E^2}{\mu^2} - 1 \right). \quad (2.18)$$

Note that the above equation describes purely radial motion in a Schwarzschild spacetime for $a = 0$.

2.1.2 Equatorial motion

For $\theta = \pi/2$ and $\dot{\theta} = 0$, the Lagrangian (2.13) becomes

$$2L_0 = \frac{(E^2/\mu^2 - \dot{r}^2) r^3 + a^2 (r + 2G_N m) E^2/\mu^2}{2r(r^2 + a^2 - 2G_N m r)} = 1, \quad (2.19)$$

which can be rewritten as

$$\frac{1}{2} \mu \dot{r}^2 - \mu \left(\frac{G_N m}{r} - \frac{a^2}{2r^2} \right) - \left(1 + \frac{2G_N m}{r} \right) \frac{a^2 E^2}{2\mu r^2} = \frac{\mu}{2} \left(\frac{E^2}{\mu^2} - 1 \right). \quad (2.20)$$

Note that the last term in the left hand side couples the energy E of the dust particle with the (specific) angular momentum a of the system.

3 Ground state and perturbative spectrum

We can discretise the rotating ball by considering an ellipsoidal core of mass $\mu_0 = \nu_0 \mu = \epsilon_0 M$ and coordinate radius $r = R_1(\tau)$ surrounded by N comoving layers of inner radius $r = R_i(\tau)$, thickness $\Delta R_i = R_{i+1} - R_i$, and mass $\mu_i = \epsilon_i M$, where ϵ_i is the fraction of ADM mass carried by the ν_i dust particles in the i^{th} layer. The gravitational mass inside the ellipsoid $r < R_i$ will be denoted by

$$M_i = \sum_{j=0}^{i-1} \mu_j = M \sum_{j=0}^{i-1} \epsilon_j , \quad (3.1)$$

with $M_1 = \mu_0$ and $M_{N+1} = M$. Likewise, we denote with A_i the specific angular momentum at the inner surface of the i^{th} layer.

The evolution of each layer can be derived by noting that dust particles located on the symmetry axis or on the equator at $r = R_i(\tau)$ will follow the geodesic equation

$$H_i \equiv \frac{P_i^2}{2\mu} - \frac{G_N \mu M_i}{R_i} + \mu W_i = \frac{\mu}{2} \left(\frac{E_i^2}{\mu^2} - 1 \right) \equiv \mathcal{E}_i , \quad (3.2)$$

where $P_i = \mu dR_i/d\tau$ is the radial momentum conjugated to $R = R_i(\tau)$, E_i the conserved momentum per unit mass conjugated to $t = t_i(\tau)$ and W_i denotes the other terms in the radial potential. In particular, for the axial motion

$$W_i = \frac{G_N M_i A_i^2}{R_i (R_i^2 + A_i^2)} \equiv W_i^{\text{ax}} , \quad (3.3)$$

whereas for equatorial motion

$$W_i = \frac{A_i^2}{2 R_i^2} \left[1 - \left(1 + \frac{2 G_N M_i}{R_i} \right) \frac{E_i^2}{\mu^2} \right] \equiv W_i^{\text{eq}} . \quad (3.4)$$

With the canonical quantization prescription $P_i \mapsto \hat{P}_i = -i\hbar \partial_{R_i}$, Eq. (3.2) becomes the time-independent Schrödinger equation

$$\hat{H}_i \psi_{n_i} = \left[-\frac{\hbar^2}{2\mu} \left(\frac{d^2}{dR_i^2} + \frac{2}{R_i} \frac{d}{dR_i} \right) - \frac{G_N \mu M_i}{R_i} + \mu W_i \right] \psi_{n_i} = \mathcal{E}_{n_i} \psi_{n_i} . \quad (3.5)$$

3.1 Non-rotating case

When $W_i \sim a^2$ is negligible, Eq. (3.5) is analogous to the equation for s -states of the hydrogen atom, and the solutions are given by the eigenfunctions

$$\psi_{n_i}(R_i) = \sqrt{\frac{\mu^6 M_i^3}{\pi \ell_p^3 m_p^9 n_i^5}} \exp\left(-\frac{\mu^2 M_i R_i}{n_i m_p^3 \ell_p}\right) L_{n_i-1}^1\left(\frac{2\mu^2 M_i R_i}{n_i m_p^3 \ell_p}\right) , \quad (3.6)$$

where L_{n-1}^1 are Laguerre polynomials and $n_i = 1, 2, \dots$, corresponding to the eigenvalues

$$\mathcal{E}_{n_i}^{(0)} = -\frac{\mu^3 M_i^2}{2 m_p^4 n_i^2} . \quad (3.7)$$

The wavefunctions (3.6) are normalised in the scalar product which makes \hat{H}_i Hermitian for $W_i = 0$, that is

$$\langle n_i | n'_i \rangle = 4\pi \int_0^\infty R_i^2 \psi_{n_i}^*(R_i) \psi_{n'_i}(R_i) dR_i = \delta_{n_i n'_i} . \quad (3.8)$$

The expectation value of the coordinate radius on these eigenstates is given by

$$\bar{R}_{n_i} \equiv \langle n_i | \hat{R}_i | n_i \rangle = \frac{3 m_p^3 \ell_p n_i^2}{2 \mu^2 M_i} , \quad (3.9)$$

with relative uncertainty

$$\frac{\overline{\Delta R}_{n_i}}{\bar{R}_{n_i}} \equiv \frac{\sqrt{\langle n_i | \hat{R}_i^2 | n_i \rangle - \bar{R}_{n_i}^2}}{\bar{R}_{n_i}} = \frac{\sqrt{n_i^2 + 2}}{3 n_i} , \quad (3.10)$$

which approaches the minimum $\overline{\Delta R}_{n_i} \simeq \bar{R}_{n_i}/3$ for $n_i \gg 1$.

By assuming that the conserved quantity E_i remains well-defined for all the dust particles in the allowed quantum states, we obtain the fundamental condition [11]

$$0 \leq \frac{E_i^2}{\mu^2} = 1 + \frac{2 \mathcal{E}_i^{(0)}}{\mu} = 1 - \frac{\mu^2 M_i^2}{m_p^4 n_i^2} , \quad (3.11)$$

which yields the lower bound for the single particle principal quantum numbers

$$n_i \geq N_i^{(0)} \equiv \frac{\mu M_i}{m_p^2} . \quad (3.12)$$

Upon saturating the above bound, one then finds

$$\bar{R}_{N_i}^{(0)} = \frac{3}{2} G_N M_i , \quad (3.13)$$

and the wavefunction for the ν_i particles in each layer is given by the same ground state

$$\psi_{N_i}^{(0)}(R_i) = \sqrt{\frac{\mu m_p}{\pi \ell_p^3 M_i^2}} \exp\left(-\frac{\mu R_i}{m_p \ell_p}\right) L_{\frac{\mu M_i}{m_p^2} - 1}^1\left(\frac{2 \mu R_i}{m_p \ell_p}\right) , \quad (3.14)$$

where the values of M_i , hence $N_i^{(0)}$ in Eq. (3.12), must be such that $\bar{R}_i^{(0)} \lesssim \bar{R}_{i+1}^{(0)}$.

3.2 Slow-rotation corrections

We can estimate the corrections to the radial potential using the above result for the ground state $E_i = 0$ with $R_i \simeq \bar{R}_{N_i}^{(0)}$. For the axial motion, we find

$$W_i^{\text{ax}} \simeq \frac{G_N M_i A_i^2}{R_i (R_i^2 + A_i^2)} \simeq \frac{8 A_i^2}{3 (9 G_N^2 M_i^2 + 4 A_i^2)} \simeq \frac{8 A_i^2}{27 G_N^2 M_i^2} , \quad (3.15)$$

whereas for equatorial motion

$$W_i^{\text{eq}} \simeq \frac{A_i^2}{2 R_i^2} \left[1 - \left(1 + \frac{2 G_N M_i}{R_i} \right) \frac{E_i^2}{\mu^2} \right] \simeq \frac{2 A_i^2}{9 G_N^2 M_i^2} . \quad (3.16)$$

For perturbation theory to apply, the above potentials must be smaller than

$$V_i = \frac{G_N M_i}{R_i} \simeq \frac{2 G_N M_i}{3 G_N M_i} \simeq \frac{2}{3} . \quad (3.17)$$

This yields

$$\frac{A_i^2}{G_N^2 M_i^2} \ll \frac{27}{12} \quad (3.18)$$

for axial motion and

$$\frac{A_i^2}{G_N^2 M_i^2} \ll 3 \quad (3.19)$$

for equatorial motion. Both conditions above are approximately satisfied for classical Kerr black holes (with $A^2 \leq G_N^2 M^2$).

Since W_i is constant to leading order in A_i , it will simply result in a shift of the energy eigenvalues

$$\mathcal{E}_i = \mathcal{E}_i^{(0)} + \mu W_i . \quad (3.20)$$

For the ground state, we then have

$$0 = \frac{E_i^2}{\mu^2} = 1 + \frac{2 \mathcal{E}_i}{\mu} = 1 - \frac{\mu^2 M_i^2}{m_p^4 N_i^2} + 2 W_i , \quad (3.21)$$

or

$$N_i \simeq \frac{\mu M_i}{m_p^2 (1 + 2 W_i)^{1/2}} \simeq \frac{\mu M_i}{m_p^2} (1 - W_i) = N_i^{(0)} (1 - W_i) . \quad (3.22)$$

Correspondingly, we obtain a reduction in the areal radius

$$\bar{R}_{N_i} = \frac{3 m_p^3 \ell_p N_i^2}{2 \mu^2 M_i} \simeq \bar{R}_{N_i}^{(0)} (1 - 2 W_i) , \quad (3.23)$$

with unaffected (leading order) uncertainty. Note in particular that

$$\bar{R}_{N_i}^{\text{ax}} < \bar{R}_{N_i}^{\text{eq}} < \bar{R}_{N_i}^{(0)} , \quad (3.24)$$

so that the effect of rotation is to reduce the coordinate radius of the layers.

This behaviour is the opposite of what was obtained in Ref. [16], where angular momentum was added to the quantum states of dust particles but assuming the Schwarzschild metric still determines the geodesic motion. For radial geodesics, the addition of angular momentum therefore amounted to a repulsive centrifugal term in the radial potential which made the size of the core increase. In the present, fully general relativistic treatment, the angular momentum is included in the background geometry and therefore affects the principal quantum number (3.23) of the ground states (3.14). Moreover, we notice that the length of a circle on the equator in the geometry (2.1) with constant t and r and $\theta = \pi/2$ is given by

$$d\ell^{\text{eq}} = r \left[1 + \frac{2 G_N m a^2}{r \rho^2} + \frac{a^2}{r^2} \right]^{1/2} d\phi , \quad (3.25)$$

which, computed for $r = \bar{R}_{N_i}^{\text{eq}}$, $m = M_i$ and $a = A_i$, yields

$$\frac{d\ell_i^{\text{eq}}}{d\phi} \simeq \bar{R}_{N_i}^{(0)} \left(1 + \frac{2 A_i^2}{27 G_N^2 M_i^2} \right) . \quad (3.26)$$

Likewise, the length of arcs at constant t , r and ϕ is given by

$$d\ell = \rho d\theta , \quad (3.27)$$

which, computed for $r = \bar{R}_{N_i}^{\text{ax}}$, $m = M_i$, $a = A_i$, around the axis of symmetry $\theta = 0$, results in

$$\frac{d\ell_i^{\text{ax}}}{d\theta} \simeq \bar{R}_{N_i}^{(0)} \left(1 - \frac{10 A_i^2}{27 G_N^2 M_i^2} \right) . \quad (3.28)$$

The above expressions show that the rotating layers are actually smaller than the spherical layers (with same M_i but $A_i = 0$) along the axis of rotation but larger on the equator. This picture agrees with the expected shape of the layers being elongated on the equatorial plane with respect to the symmetry axis in spherical coordinates, which are the ones used to express the states (3.14).

3.2.1 Core size

For the outermost layer (the surface of the core), we have

$$R_s \simeq \frac{4}{3} \bar{R}_{N_N} \simeq \frac{3}{2} G_N M (1 - 2 W_N) , \quad (3.29)$$

so that along the axis of symmetry

$$R_s^{\text{ax}} \simeq \frac{3}{2} G_N M \left(1 - \frac{8 A^2}{27 G_N^2 M^2} \right) , \quad (3.30)$$

where A is the constant specific angular momentum of the outer Kerr geometry. On the equatorial plane one similarly finds

$$R_s^{\text{eq}} \simeq \frac{3}{2} G_N M \left(1 - \frac{2 A^2}{9 G_N^2 M^2} \right) , \quad (3.31)$$

so that

$$\frac{R_s^{\text{eq}}}{R_s^{\text{ax}}} \simeq 1 - 2 W_N^{\text{eq}} + 2 W_N^{\text{ax}} \simeq 1 + \frac{2 A^2}{27 G_N^2 M^2} . \quad (3.32)$$

It is particularly interesting to compare the above results with the horizons (2.4) of the (slowly rotating) external Kerr geometry,

$$R_{\pm} \simeq G_N M \pm G_N M \left(1 - \frac{A^2}{2 G_N^2 M^2} \right) . \quad (3.33)$$

From Fig. 1, we see that both core radii are larger than R_- for all $A^2 \leq G_N^2 M^2$. The equatorial core radius remains shorter than R_+ for small rotation and until $R_s^{\text{eq}} \simeq R_+$ for

$$\frac{A^2}{G_N^2 M^2} \simeq \frac{3}{2} \left(\sqrt{7} - 2 \right) \simeq 0.984 , \quad (3.34)$$

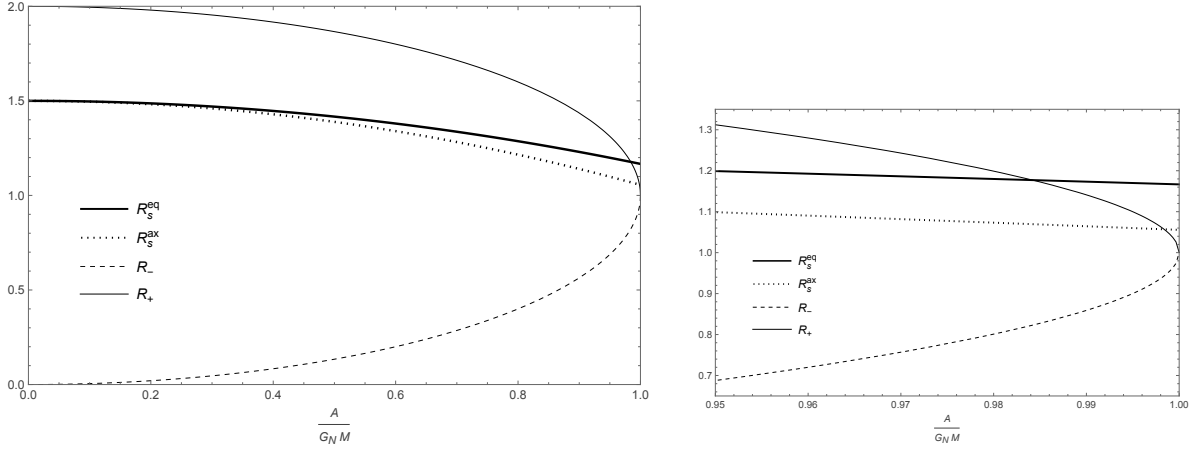


Figure 1: Core radii vs horizon radii for the whole range of classical Kerr black holes $A^2 \leq G_N^2 M^2$ (left panel); right panel shows the region of near extremal rotation magnified.

whereas the axial radius $R_s^{\text{ax}} \simeq R_+$ for

$$\frac{A^2}{G_N^2 M^2} \simeq \frac{3}{2} \left(\sqrt{73} - 5 \right) \simeq 0.998 . \quad (3.35)$$

Clearly, both of these values of the specific angular momentum are way outside the regime of slow rotation and should not be trusted.

3.2.2 Near extremal rotation

Let us consider the near extremal case for which $A_i^2 \simeq G_N^2 M_i^2$. For the axial motion, we find

$$W_i^{\text{ax}} \simeq \frac{G_N M_i A_i^2}{R_i (R_i^2 + A_i^2)} \simeq \frac{8 A_i^2}{3 (9 G_N^2 M_i^2 + 4 A_i^2)} \simeq \frac{8}{39} , \quad (3.36)$$

whereas for equatorial motion

$$W_i^{\text{eq}} \simeq \frac{A_i^2}{2 R_i^2} \simeq \frac{2}{9} . \quad (3.37)$$

As noted before, these values are smaller than V_i in Eq. (3.17) so that previous perturbative results should still provide at least a qualitatively valid picture in the whole classical range.

3.3 Quantum rotating core

In the classical description, each dust layer can be made arbitrarily thin. However, in the quantum description described above, we can assume the minimum thickness is given by the uncertainty $\Delta \bar{R}_{n_i} \sim \bar{R}_{n_i}/3$ obtained from Eq. (3.10) for $n_i \gg 1$ [10]. In the global ground state formed by layers in their own ground state we then have

$$\bar{R}_{N_{i+1}} = \bar{R}_{N_{i+1}}^{(0)} (1 - 2 W_{i+1}) = \bar{R}_{N_i} + \Delta \bar{R}_{n_i} \simeq \frac{4}{3} \bar{R}_{N_i}^{(0)} (1 - 2 W_i) . \quad (3.38)$$

From Eq. (3.23), we obtain

$$\frac{3\ell_p M_{i+1}}{2m_p} (1 - 2W_{i+1}) \simeq \frac{2\ell_p M_i}{m_p} (1 - 2W_i) , \quad (3.39)$$

and the (discrete) mass function M_i therefore depends on the angular momentum A_i . In particular, on the symmetry axis, we have

$$M_{i+1}^{\text{ax}} \left(1 - \frac{16 A_{i+1}^2}{27 G_N^2 (M_{i+1}^{\text{ax}})^2} \right) \simeq \frac{4}{3} M_i^{\text{ax}} \left(1 - \frac{16 A_i^2}{27 G_N^2 (M_i^{\text{ax}})^2} \right) , \quad (3.40)$$

whereas

$$M_{i+1}^{\text{eq}} \left(1 - \frac{4 A_{i+1}^2}{9 G_N^2 (M_{i+1}^{\text{eq}})^2} \right) \simeq \frac{4}{3} M_i^{\text{eq}} \left(1 - \frac{4 A_i^2}{9 G_N^2 (M_i^{\text{eq}})^2} \right) , \quad (3.41)$$

on the equator.

From the general discussion in Ref. [3], we know that the inner Cauchy horizon is not present if the mass function and specific angular momentum $m \sim a \sim r$. Let us therefore assume that the specific angular momentum A_i is linearly dependent on the radius R_i ,

$$A_i \propto \bar{R}_i \simeq \alpha \bar{R}_i^{(0)} . \quad (3.42)$$

From Eqs. (3.15) and (3.16), the perturbations become

$$W_i^{\text{ax}} \simeq \frac{2\alpha^2}{3(1+\alpha^2)} \simeq \frac{2}{3}\alpha^2 \quad (3.43)$$

and

$$W_i^{\text{eq}} \simeq \frac{1}{2}\alpha^2 , \quad (3.44)$$

at leading order in the constant α , which is of the same order of magnitude of the slow-rotation parameter $A_i/G_N M_i$. With this assumption, both Eqs. (3.40) and (3.41) therefore simplify to

$$M_{i+1}^{\text{ax}/\text{eq}} \simeq \frac{4}{3} M_i^{\text{ax}/\text{eq}} , \quad (3.45)$$

which is precisely the linear behaviour found in the spherically symmetric case. In fact, given the total ADM mass M , the mass distribution within each layer is then determined by

$$M_i^{\text{ax}/\text{eq}} \simeq \left(\frac{3}{4} \right)^{N+1-i} M \equiv M_i , \quad (3.46)$$

which implies that the quantum states with specific angular momentum given in Eq. (3.42) correspond to a mass function that grows linearly with the layer size, that is

$$M_i \simeq \frac{2}{3} (1 + \alpha^2) \frac{\bar{R}_{N_i}^{\text{eq}}}{G_N} \simeq \frac{2}{3} \left(1 + \frac{4}{3} \alpha^2 \right) \frac{\bar{R}_{N_i}^{\text{ax}}}{G_N} . \quad (3.47)$$

We remark that this configuration is also consistent with the ellipsoidal shape of the collapsed cores described by Eqs. (3.24), (3.26) and (3.28).

For the above reasons, we will limit our following analysis to the case with linearly growing specific angular momentum (3.42) and mass function (3.47).

3.4 Angular momentum and horizon quantisation

According to Eq. (3.22), the ground state of dust particles in each layer is (approximately) given by spherical wavefunctions (3.14) with different quantum numbers along the axis of symmetry and on the equatorial plane, namely

$$N_i^{\text{eq}} \simeq \frac{\mu M_i}{m_p^2} \left(1 - \frac{1}{2} \alpha^2\right) < N_i^{\text{ax}} \simeq \frac{\mu M_i}{m_p^2} \left(1 - \frac{2}{3} \alpha^2\right). \quad (3.48)$$

Since N_i^{ax} and N_i^{eq} are integers, one obtains that the specific angular momentum must satisfy the quantisation rule

$$N_i^{\text{ax}} - N_i^{\text{eq}} \simeq \left(\frac{3}{4}\right)^{N+1-i} \frac{\mu M}{6 m_p^2} \alpha^2. \quad (3.49)$$

For $i = N + 1$, one obtains $M_i = M$ and

$$\alpha^2 \simeq \frac{6 m_p^2}{\mu M} (N_{N+1}^{\text{ax}} - N_{N+1}^{\text{eq}}), \quad (3.50)$$

so that Eq. (3.42) implies the quantisation of the specific angular momentum in the exterior Kerr geometry

$$A^2 \simeq \left(\alpha R_s^{(0)}\right)^2 \simeq \frac{27 M}{2 \mu} \ell_p^2 (N_{N+1}^{\text{ax}} - N_{N+1}^{\text{eq}}), \quad (3.51)$$

where we recall that $R_s^{(0)} \simeq 3 G_N M / 2$.

From Eq. (3.29), we also find

$$\alpha^2 \simeq \frac{R_s^{\text{eq}} - R_s^{\text{ax}}}{2 G_N M} \simeq \frac{3 (R_s^{\text{eq}} - R_s^{\text{ax}})}{4 R_s^{(0)}}, \quad (3.52)$$

which implies

$$\frac{R_s^{\text{eq}} - R_s^{\text{ax}}}{R_s^{(0)}} \simeq \frac{24 m_p^4}{\mu^2 M^2} (N_{N+1}^{\text{ax}} - N_{N+1}^{\text{eq}}), \quad (3.53)$$

so that the shape of the core is also quantised.

The outer horizon area in the Kerr geometry is given by

$$\mathcal{A}_H = 4\pi (R_+^2 + A^2) \simeq 4\pi \left(R_s^{(0)}\right)^2 \left(1 - \frac{3}{4} \alpha^2\right). \quad (3.54)$$

From the quantisation of the spherical dust core [10],

$$\frac{M}{\mu} N_{N+1}^{(0)} \simeq \frac{M^2}{m_p^2}, \quad (3.55)$$

we then find

$$\mathcal{A}_H \simeq 4\pi \ell_p^2 \frac{M}{\mu} N_{N+1}^{(0)} \left[1 - \frac{9 m_p^2}{2 \mu M} (N_{N+1}^{\text{ax}} - N_{N+1}^{\text{eq}})\right], \quad (3.56)$$

where we remark that M/μ is not necessarily an integer.

3.5 Effective interior geometry

We have seen that, for a core characterised by the linear relation (3.42) for the specific angular momentum, the mass function $M_i^{\text{ax}} \simeq M_i^{\text{eq}} \equiv M_i \propto \bar{R}_i^{(0)}$. It then follows that the corresponding effective metric can be simply obtained by applying the Gurses and Gursey algorithm [18] (generalised in Ref. [3]) with a seed geometry provided by the spherically symmetric case of non-rotating dust described in Refs. [10, 19] and specific angular momentum (3.42). This is all consistent with the initial assumption of a metric of the form in Eq. (2.1), where $m = m(r)$ and $a = a(r)$ are now determined by the ground states of the layers.

The explicit form of the metric function $\Delta = \Delta(r)$ in Eq. (2.3) for the ground state is particularly interesting since it allows us to verify that a Cauchy horizon never appears. For this analysis, we will consider two effective mass functions, $m = m_{\text{par}}(r)$ and $m = m_{\text{int}}(r)$, which interpolate between the interior discrete mass distribution M_i and the outer Kerr metric with constant M (for more details see also Ref. [19]). In particular,

$$m_{\text{int}} = c_i r , \quad \text{for } 0 \leq r < \bar{R}_{N_N}^{(0)} , \quad (3.57)$$

where the constant

$$c_i = \frac{M_N}{\bar{R}_{N_N}^{(0)}} \simeq \frac{2 m_p}{3 \ell_p} , \quad (3.58)$$

and the analytic expression inside the outermost layer $\bar{R}_{N_N}^{(0)} < r < R_s$ is given in Eq. (A.2) of Appendix A.

The function m_{par} is a parabolic profile which matches the outer constant ADM mass M for $r \rightarrow \infty$, and was introduced in Ref. [14] as an improvement over m_{int} to better account for the spatial overlapping of the wavefunctions (3.14). Its analytic expression is recalled in Eq. (A.3), from which we have

$$m_{\text{par}} = c_p r + \mathcal{O}(r^2) , \quad \text{for } r \rightarrow 0^+ , \quad (3.59)$$

with

$$c_p = \frac{\bar{a} m_p}{2 \ell_p} \quad (3.60)$$

and the fitting parameter $\bar{a} \simeq 1.53$.

The effective angular momentum $a = a(r)$ in Eq. (2.1) can be obtained from the above mass functions by noting that Eqs. (3.42) and (3.47) imply

$$\frac{A_i}{A} \simeq \frac{\bar{R}_{N_i}^{(0)}}{\bar{R}_s^{(0)}} \simeq \frac{M_i}{M} , \quad (3.61)$$

so that

$$a(r) = A \frac{m(r)}{M} . \quad (3.62)$$

The function $\Delta = \Delta(r)$ is shown in Fig. 2. In agreement with the general analysis of Ref. [3], we see that $\Delta(0) = 0$ and there is a unique zero $r_H > 0$ for values of the specific angular momentum within the range

$$0 < \frac{A}{G_N M} < \delta_i \equiv \frac{3}{2\sqrt{3}} < 1 , \quad (3.63)$$

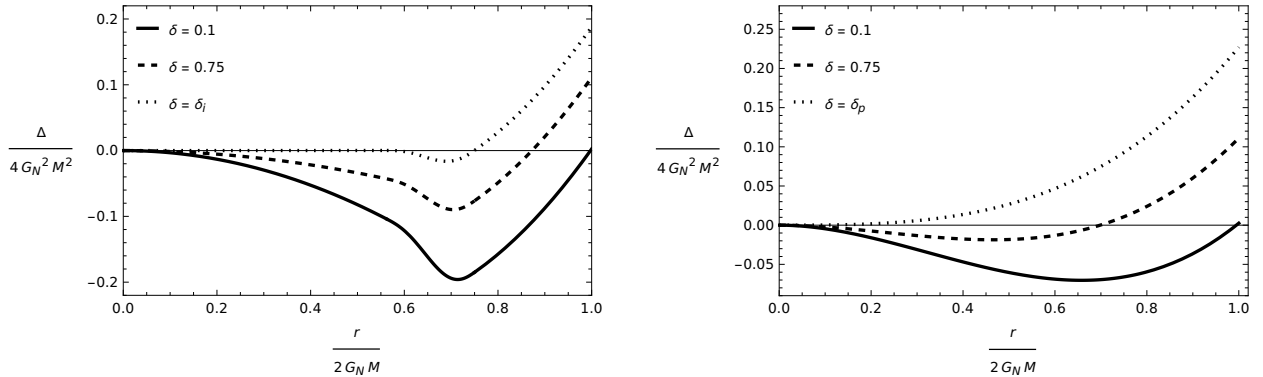


Figure 2: Function Δ in Eq. (2.3) for m_{int} (left panel) and m_{par} (right panel) for different values of $\delta = A/G_N M$, with $M = 150 m_p$. The dotted lines correspond to the maximum values $\delta_i \simeq 0.867$ (left panel) and $\delta_p \simeq 0.953$ (right panel).

for $m = m_{\text{int}}(r)$, and

$$0 < \frac{A}{G_N M} < \delta_p \equiv 2 \sqrt{\frac{\bar{a} - 1}{\bar{a}^2}} < 1 , \quad (3.64)$$

for $m = m_{\text{par}}(r)$. For the critical values $\delta = \delta_i$ or $\delta = \delta_p$ the radius $r_H = 0$.

Note that both ranges in Eqs. (3.63) and (3.64) impose stronger requirements on $A/G_N M$ for the existence of the horizon than the limits of the perturbative regime given in Eqs. (3.18) and (3.19). In particular, this analysis for m_{int} and m_{par} excludes classical near-extremal configurations with $A \simeq G_N M$.

4 Conclusions and outlook

In this work we extended the quantisation of the layered dust core [10] to rotating (ellipsoidal) cores, where dust particles move along time-like geodesics of the (generalised) Kerr geometry (2.1), improving the description given in Ref. [16]. In that previous work, particles fall freely along geodesics in the Schwarzschild spacetime, and their rotation was only approximately described by states with non-zero angular momentum, hence neglecting the general-relativistic features of the Kerr geometry.

If we only consider motion along the rotation axis or on the equator, the Hamiltonian constraint (3.5) reduces to the expression for the spherically symmetric distribution, described in detail in [10, 11], with an additional term $W_i \sim a^2/G_N^2 M^2$ which can be treated as a perturbation. The global ground state is described by ellipsoidal layers elongated on the equator with respect to the rotation axis. In the perturbative regime of (relatively) slow-rotation, the equatorial radius R_s^{eq} is always shorter than the outer horizon R_+ , thus describing a black hole, whereas a configuration with $R_s^{\text{ax/eq}} \simeq R_+$ cannot be described within this perturbative approach. We remark that the results obtained in this work improve on the analysis of Ref. [16] by including the angular momentum in the generalised Kerr geometry that determines the geodesics.

A possible ground state appears to be described by a configuration in which $A_i \propto \bar{R}_i \propto M_i$, as described in Section 3.3. In fact, this condition ensures that no Cauchy horizon ever forms within the core and that the central ring-singularity is replaced by an integrable singularity. In

this configuration, the specific angular momentum A_i is quantized according to Eq. (3.49), which ensures the quantisation of the specific angular momentum A in the exterior solution, in agreement with Ref. [16]. Together with the quantisation of the spherical dust core, this result implies that the outer horizon area is quantised in Plank units. Remarkably, in this configuration the effective metric can be determined from the spherically symmetric non-rotating dust distribution given in Refs. [10,11,14]. In Section 3.5, we analysed the effective causal structure inside the core by means of the function $\Delta = \Delta(r)$, which is computed for specific seed mass distributions described in Ref. [19]. The absence of a Cauchy horizon and the existence of the only event horizon at $r = r_H$, within the slow-rotation limits given by Eqs. (3.63) and (3.64), is in agreement with the general picture that quantum matter should be able to regularise the interior region of black holes [3].

Acknowledgments

T.B. and R.C. are partially supported by the INFN grant FLAG. The work of R.C. has also been carried out in the framework of activities of the National Group of Mathematical Physics (GNFM, INdAM) and the COST action CA23115 (RQI).

A Effective mass functions

We show here the explicit forms of the continuous MSH mass functions used in Section 3.5. More details can be found in Ref. [19].

The mass function $m = m_{\text{int}}(r)$ simply interpolates between the linear behaviour $M_i \propto \bar{R}_i$ up to the inner radius of the outermost layer and the constant ADM mass M outside the core,

$$m_{\text{int}} = \begin{cases} c_i r, & \text{for } r \leq \bar{R}_{N_N}^{(0)} \\ B(r), & \text{for } \bar{R}_{N_N}^{(0)} \leq r \leq R_s^{(0)} = \frac{4}{3} \bar{R}_{N_N}^{(0)} \\ M, & \text{for } r \geq R_s^{(0)}. \end{cases} \quad (\text{A.1})$$

The interpolating function is given by the 5-th order polynomial

$$\begin{aligned} B = & -\frac{c_1}{\Delta x^3} (x - x_1)^3 + \frac{M}{\Delta x^3} (x - x_0)^3 - \left(\frac{3c_1}{\Delta x^4} + \frac{c_2}{\Delta x^3} \right) (x - x_1)^3 (x - x_0) \\ & - \frac{3M}{\Delta x^4} (x - x_0)^3 (x - x_1) - \left(\frac{6c_1}{\Delta x^5} + \frac{3c_2}{\Delta x^4} \right) (x - x_1)^3 (x - x_0)^2 \\ & + \frac{6M}{\Delta x^5} (x - x_1)^2 (x - x_0)^3, \end{aligned} \quad (\text{A.2})$$

where $x \equiv r/2G_N M$, $c_1 = M_N$, $c_2 = c_1 (2G_N M/\bar{R}_{N_N}^{(0)})$, and the width of the outermost layer is denoted by $\Delta x = (R_s^{(0)} - \bar{R}_{N_N}^{(0)})/2G_N M = 1/4$.

The wavefunctions of dust particles (3.14) do not vanish outside the respective layers, which yields a non-zero probability that at least the nearest layers overlap. To account for this effect, the mass function $m = m_{\text{par}}(r)$ was computed in Ref. [14] for the spherically symmetric case and is given by

$$m_{\text{par}} = M (\bar{a} x + \bar{b} x^{\bar{c}}), \quad (\text{A.3})$$

with $x \equiv r/2G_N M$ and the fitting coefficients

$$\bar{a} = 1.53, \quad \bar{b} = -0.533, \quad \bar{c} = 1.90. \quad (\text{A.4})$$

These values were used for the plots in the right panel of Fig. 2.

References

- [1] S. W. Hawking and G. F. R. Ellis, “The Large Scale Structure of Space-Time,” (Cambridge University Press, Cambridge, 1973)
- [2] R. Carballo-Rubio, F. Di Filippo, S. Liberati and M. Visser, “Singularity-free gravitational collapse: From regular black holes to horizonless objects,” [arXiv:2302.00028 [gr-qc]].
- [3] R. Casadio, A. Giusti and J. Ovalle, JHEP **05** (2023) 118 [arXiv:2303.02713 [gr-qc]].
- [4] C. W. Misner and D. H. Sharp, Phys. Rev. **136** (1964), B571.
- [5] W. C. Hernandez and C. W. Misner, Astrophys. J. **143** (1966) 452.
- [6] R. Casadio, Int. J. Mod. Phys. D **31** (2022) 2250128 [arXiv:2103.00183 [gr-qc]].
- [7] R. Casadio, A. Giusti and J. Ovalle, Phys. Rev. D **105** (2022) 124026 [arXiv:2203.03252 [gr-qc]].
- [8] V. N. Lukash and V. N. Strokov, Int. J. Mod. Phys. A **28** (2013) 1350007 [arXiv:1301.5544 [gr-qc]].
- [9] J. R. Oppenheimer and H. Snyder, Phys. Rev. **56** (1939) 455.
- [10] R. Casadio, Phys. Lett. B **843** (2023) 138055 [arXiv:2304.06816 [gr-qc]].
- [11] R. Casadio, Eur. Phys. J. C **82** (2022) 10 [arXiv:2103.14582 [gr-qc]].
- [12] R. Casadio, R. da Rocha, P. Meert, L. Tabarroni and W. Barreto, Class. Quant. Grav. **40** (2023) 075014 [arXiv:2206.10398 [gr-qc]].
- [13] R. C. Tolman, Proc. Nat. Acad. Sci. **20** (1934) 169.
- [14] L. Gallerani, A. Mentrelli, A. Giusti and R. Casadio, Int. J. Mod. Phys. D **34** (2025) 2550035 [arXiv:2501.07219 [gr-qc]].
- [15] R. Casadio, R. da Rocha, A. Giusti and P. Meert, Phys. Rev. D **110** (2024) 104067 [arXiv:2407.04146 [gr-qc]].
- [16] R. Casadio and L. Tabarroni, Eur. Phys. J. Plus **138** (2023) 104 [arXiv:2212.05514 [gr-qc]].
- [17] R. L. Arnowitt, S. Deser and C. W. Misner, Phys. Rev. **116** (1959) 1322.
- [18] M. Gurses and F. Gursey, J. Math. Phys. **16** (1975) 2385.
- [19] T. Bambagiotti, L. Gallerani, A. Mentrelli, A. Giusti and R. Casadio, “Quantum dust cores of black holes and their quasi-normal modes,” [arXiv:2509.01570 [gr-qc]].